UKACC International Conference on Control 2012
Cardiff, UK, 3-5 September 2012

IMAGE RESOLUTION ENHANCEMENT USING MULTI-WAVELET AND CYCLE-SPINNING

P. Bagheri Zadeh, A. Sheikh Akbari

Faculty of Computing, Engineering and Technology, Staffordshire University, Staford, UK
E-mails: (p.bagheri-zadeh, a.s.akbari)@staffs.ac.uk

Keywords: Super-resolution, multi-wavelets, cycle-spinning.

Abstract

In this paper a multi-wavelet and cycle-spinning based image resolution enhancement technique is presented. The proposed technique generates a high-resolution image for the input low-resolution image using the input image and an inverse multi-wavelet transform (all multi-wavelet high frequency subbands' coefficients are set to zero). The concept of the cycle spinning algorithm in conjunction with the multi-wavelet transform is then used to generate a high quality super-resolution image for the input image from the resulting high resolution image, as follows: A number of replicated images with different spatial shifts from the resulting high-resolution image is first generated; Each of the replicated images is de-correlated into its subbands using a multi-wavelet transform; The multi-wavelet high frequency subbands' coefficients of each of the de-correlated images are set to zero and then a primary super-resolution image for each of these images is produced using an inverse multi-wavelet transform; The resulting primary super-resolution images are then spatially shift compensated and the output super-resolution image is created by averaging the resulting shift compensated images. Experimental results were generated using four standard test images and compared to the state of art techniques. Results show that the proposed technique significantly outperforms the classical and non-classical super-resolution methods both subjectively and objectively.

1 Introduction

The Super-Resolution (SR) techniques aim at displaying or printing an image at a resolution higher than that the original image without severely affecting the visual quality of the image. Since natural images exhibit abrupt discontinuities at object boundaries, traditional image interpolation methods such as linear and higher-order polynomial interpolation algorithms (which implicitly assume the underlying image is locally smooth) may not be able to offer the required visual quality [1].

Wavelets have been applied to image resolution enhancement to address the over smoothing problem of the traditional super-resolution techniques and promising results have been reported in the literature [2, 4, 7, 8, 9, 10]. The common feature of the wavelet based techniques is the assumption that the image to be enhanced is the wavelet approximation band of the high-resolution image. These techniques generate the high frequency wavelet coefficients from the given low resolution image [9]. A wavelet-based interpolation method was proposed by Carey et al. in [1]. Their proposed method estimates the wavelet high frequency coefficients of the image by exploiting the regularity of edges across the scales. They reported promising results. However, this method may not be able to estimate wavelet high-frequency coefficients with small values. A wavelet based image resolution enhancement algorithm using an adapted cycle-spinning technique was reported in [8]. This algorithm uses the information in the low-resolution image wavelet subbands to estimate the local edge orientation of the image. This local edge orientation information is then used to determine the cycle spinning parameters to generate the enlarged image. Authors reported superior results compared to Kinebuchi and Muresan method. Temizel and Vlachos proposed another wavelet based image resolution enhancement using cycle-spinning [7], which gives superior results to the state of the art. Another wavelet based image resolution enhancement algorithm, which operates in a quad-tree wavelet decomposition framework and exploits wavelet coefficient correlation in a local neighbourhood sense, was presented in [9]. This method employed linear least-squares regression algorithm to estimate the wavelet high-frequency coefficients. This method gives superior results compared to the conventional methods for a wide range of test images. Another image resolution enhancement method in wavelet domain using inter-subband correlation was presented by Piao et al. [4]. They designed filters to estimate high frequency subbands from the lower bands. They reported superior results, up to 0.36dB, to the competing methods.

Wavelets filters generally have poor frequency characteristic. Hence, wavelet baseband of the images usually contain some of the image high-frequency information [4]. This property of the wavelets is usually used to improve the quality of the enlarged image especially around their edges. Applications of multi-wavelet transform [6] that use two or more wavelets in image decomposition generate four or more approximation bands from the input image. Similar to wavelets, multi-wavelet filters also have poor frequency characteristics. Therefore, their resulting approximation bands carry different high-frequency information of the image. This feature of multi-wavelets makes them a potential tool in enhancing image resolution. The application of multi-wavelets in enlarging images and also application of cycle spinning algorithm in multi-wavelet domain for enlarging images have

not been reported in the literature. Hence, in this paper, cycle-spinning algorithm is adapted into multi-wavelet domain and used for enlarging images. The rest of the paper is organized as follows: In Section 2, a brief review of the multi-wavelet transform is presented. The proposed image resolution enhancement technique is discussed in Section 3. Experimental results are presented in Section 4. Finally the paper is concluded at Section 5.

2 Multi-wavelet transform

Multi-wavelet transforms are very similar to scalar wavelet transforms with some vital differences. Classical wavelet theory is based on the following refinement equations:

$$\phi(t) = \sum_{k=-\infty}^{k=\infty} h_k \phi(mt-k)$$
$$\psi(t) = \sum_{k=-\infty}^{k=\infty} g_k \psi(mt-k) \qquad (1)$$

where $\phi(t)$ is a scaling function, $\psi(t)$ is a wavelet function, h_k and g_k are scalar filters, m represents the subband number and k is the shifting parameter. In contrast to wavelet transforms, multi-wavelets have two or more scaling and wavelet functions. The set of scaling and wavelet functions of a multi-wavelet in vector notation can be defined as:

$$\Phi(t) \equiv [\phi_1(t) \quad \phi_2(t) \quad \phi_3(t) \quad \ldots \quad \phi_r(t)]^T$$
$$\Psi(t) \equiv [\psi_1(t) \quad \psi_2(t) \quad \psi_3(t) \quad \ldots \quad \psi_r(t)]^T \qquad (2)$$

where $\Phi(t)$ and $\Psi(t)$ are the multi-scaling and multi-wavelet functions, respectively, with r scaling- and wavelet-functions. In the case of scalar wavelets their multiplicity order r is equal to 1, while multi-wavelets support $r \geq 2$. To date, most multi-wavelets have multiplicity order, $r = 2$. A multi-wavelet with two scaling and wavelet functions can be defined as [6]:

$$\Phi(t) = \sqrt{2} \sum_{k=-\infty}^{k=\infty} H_k \Phi(mt-k)$$
$$\Psi(t) = \sqrt{2} \sum_{k=-\infty}^{k=\infty} G_k \Psi(mt-k) \qquad (3)$$

where H_k and G_k are 2×2, ($r\times r$), matrix filters and m is the subband number. Similar to wavelet transforms, multi-wavelets can be implemented using Mallat's filter bank theory [3]. A visual comparison of the resulting subbands for a 2D wavelet and respectively multi-wavelet, is shown in Figures 1(a) and 1(b). From Figure 1, the multi-wavelet transform generates four subbands instead of each subband created by the wavelet transform, and these four subbands carry different spectral content of the input image due to the properties of multi-wavelet filters.

The major advantage of multi-wavelets over scalar wavelets is their ability to possess symmetry, orthogonality and higher

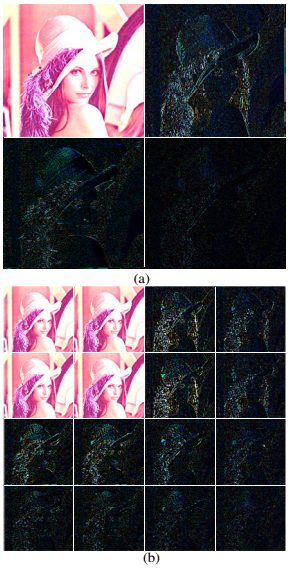

Figure 1: Single level decomposition of Lena test image (a) Antonini 9/7 wavelet transform, (b) balanced bat01 multiwavelet transform.

order of approximation simultaneously, which is not possible for scalar wavelets. Furthermore, the multi-channel structure of the multi-wavelet transform is a closer approximation to the human visual system than what wavelets offer. These features of multi-wavelets make them a potential tool in enhancing image resolution. Further information about the generation of multi-wavelets, their properties and their applications can be found in [5, 6].

3 Multi-wavelet based image resolution enhancement technique

Figure 2 shows a block diagram of the proposed multi-wavelet based image resolution enhancement technique. A low resolution image is input to the system. The input image coefficients are weighted to generate four multi-wavelet basebands. The weighting factor for each of the multi-wavelet basebands equals to the overall multi-wavelet filters gain for that subband. The Inverse Multi-Wavelet Transform (IMWT) block produces a High-Resolution (HR) image for the input image using the information in the resulting basebands (the coefficients in multi-wavelet high frequency subbands are set to zero.). The concept of the cycle spinning technique is then combined with the multi-wavelet transform to generate a super-resolution image for the input image from the resulting HR-image, as follows: The resulting HR-image is first spatially shifted with different 2D shift values, generating N Shifted High Resolution (SHR) images. Then the N 2D-shift vectors are determined using equation 4:

$$\begin{bmatrix} (-k,-k) & (-k,-k+1) & \cdots & (-k,k) \\ (-k+1,-k) & (-k+1,-k+1) & \cdots & (-k+1,k) \\ \cdots & \cdots & \cdots & \cdots \\ (k,-k) & (k,-k+1) & \cdots & (k,\ k) \end{bmatrix} \qquad (4)$$

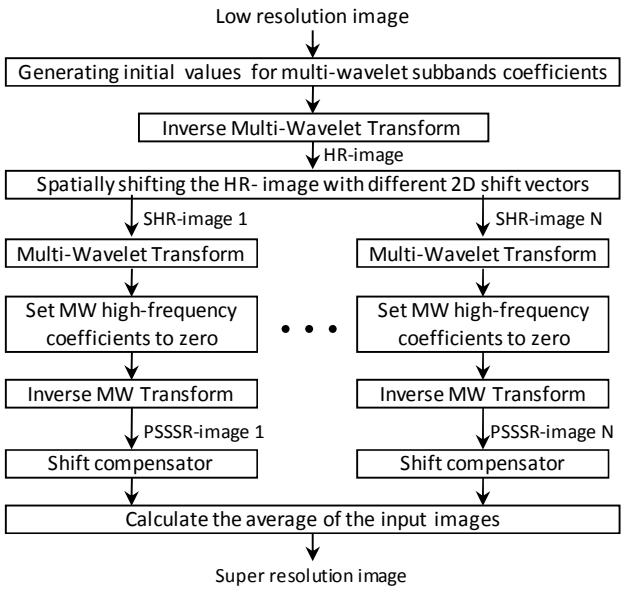

Figure 2: Block diagram of the multi-wavelet based image enlargement algorithm.

where k is the maximum number of pixel shifts in both horizontal and vertical directions. In this paper k was set to 3, as system exhibits its best performance with this value. Number of shifted images, N, can be calculated using equation 5:

$$N = (2k + 1)^2 \qquad (5)$$

where k is the maximum number of pixel shifts in both horizontal and vertical directions.

Each of the resulting N Shifted High Resolution (SHR) images is then processed as follows: I) a 2D Multi-Wavelet Transform (MWT) is applied on the SHR-image, de-correlating the SHR-image into its multi-wavelet subbands; II) the coefficients in the resulting multi-wavelet high frequency subbands are set to zero; III) a 2D Inverse Multi-Wavelet Transform (IMWT) is used to generate a Primary Spatially Shifted Super Resolution (PSSSR) image from the resulting coefficients; IV) the PSSSR-image is spatially inverse shifted, bringing back the image coefficients onto its original positions.

The output super-resolution image is created by averaging the resulting N-shift compensated PSSSR-images.

4 Experimental results

To generate experimental results, four standard test images called: Lena, Elaine, Baboon and Peppers are taken. Each of these four images, is first lowpass filtered using a 2D Blackman filter, and then down sampled by a factor of 2 in both horizontal and vertical directions, generating a replica low resolution image for each of them. The Blackman 2D FIR filter coefficients are tabulated in Table 1.

0.0381	0.1051	0.0381
0.1051	0.4273	0.1051
0.0381	0.1051	0.0381

Table 1: The Blackman 2D FIR filter coefficients.

To evaluate the performance of the proposed method, the resulting low resolution Lena, Elaine, Baboon and Peppers test images are enlarged using the proposed method, Nearest-neighbourhood, Bilinear, Bicubic, Sinc, Cycle Spinning (CS) [8], Directional Cycle Spinning (DSC) [9], and Yinji [4] methods. In this research, ghm multi-wavelet was used to generate the experimental results. The Peak Signal to Noise Ratio (PSNR) measurements for the enlarged images were calculated and tabulated in Table 2.

	Lena	Elaine	Pepper	Baboon
Nearest	29.15	30.15	29.20	25.30
Bilinear	29.90	30.45	29.69	26.28
Bicubic	30.25	30.59	29.90	26.91
Sinc	34.49	32.89	33.26	31.55
Yinji	33.75	32.50	32.79	30.17
CS	34.31	32.92	33.22	31.16
DCS	34.77	33.19	33.54	32.16
Proposed	34.96	33.35	33.63	32.55

Table 2: The PSNR comparison of different methods.

From table 2, it can be seen that the proposed method outperforms the competing methods when enlarging the images that contain significant high frequency information. The proposed technique produces almost the same objective quality when enlarging images containing less high frequency components.

To give a visual perception of the resulting enlarged images, original Lena test image and its enlarged image using the proposed technique are shown in Figure 3. From Figure 3, it can be seen that the enlarged image is almost the same as the original image and it is hard to differentiate between the original and the enlarged image.

To facilitate the assessment of different enlargement techniques, the enlarged image using the proposed method, Nearest neighbourhood, Bilinear, Bicubic, Sinc, Cycle Spinning (CS), Directional Cycle Spinning (DSC), and Yinji methods are subtracted from the ground truth image and magnified by a factor of 10 (shown in Figure 4). From these figures it is obvious that the proposed technique exhibits the lowest residuals compared to the other techniques.

(a) (b)

Figure 3: a) Original Lena test image; b) enlarged Lena test image using the proposed technique.

4 Conclusions

In this paper, a new image resolution enhancement technique was proposed. The proposed technique adopts the cycle-spinning scheme into multi-wavelet domain, increasing the quality of the enlarged images. Experiments on natural test images showed the proposed technique outperforms the state of the art techniques especially when the enlarged images contain high frequency information.

References

[1] W.K. Carey, D.B. Chuang and S.S. Hemami, "Regularity preserving Image Interpolation, " *IEEE Trans. on Image Process*, **volume 8**, pp.1295-1297, (Sep. 1999).

[2] K. Kinebuchi, D. D.Muresan, T. W. Parks, "Image interpolation using wavelet-based hidden Markov trees," in *Proc. ICASSP 2001*, pp. 1957-1960, (May 2001).

[3] S. Mallat, *A Wavelet Tour of Signal Processing*, Academic Press, (1999).

[4] Y. Piao , L. H. Shin and H. W. Park, "Image Resolution Enhancement using Inter-Subband Correlation in Wavelet Domain," in *Proc. IEEE Int. conf. on Image processing*, pp. 445-448, (September 2007).

[5] V. Strela and A.T. Walden, "Signal and image denoising via wavelet thresholding: orthogonal and biorthogonal, scalar and multiple wavelet transforms," *In Nonlinear and Nonstationary Signal Process.*, pp. 124-157, (1998).

[6] V. Strela, "Multiwavelets: theory and applications," PhD thesis, MIT, (1996).

[7] A. Temizel and T. Vlachos, "Wavelet Domain Image Resolution Enhancement using Cycle-spinning," *Electronics Letters*, **volume 41,** No.3, (Feb. 2005).

[8] A. Temizel and T. Vlachos, "Image resolution up-scaling in the wavelet domain using directional cycle spinning," *Jour. of Electronic Imaging*, **volume 14(4),** (Dec. 2005).

[9] A. Temizel and T. Vlachos, "Wavelet Domain Image Resolution Enhancement," IEE *Proc. Vis. Image Signal Processing*, **volume 153,** No.1, pp. 25-30, (Feb. 2006).

[10] D.H. Woo, I.K. Eom and Y.S. Kim, "Image Interpolation Based on Inter-scale Dependency in Wavelet Domain," in *Proc. IEEE Int. conf. on Image processing,* pp. 1687-1690, (October 2004,).

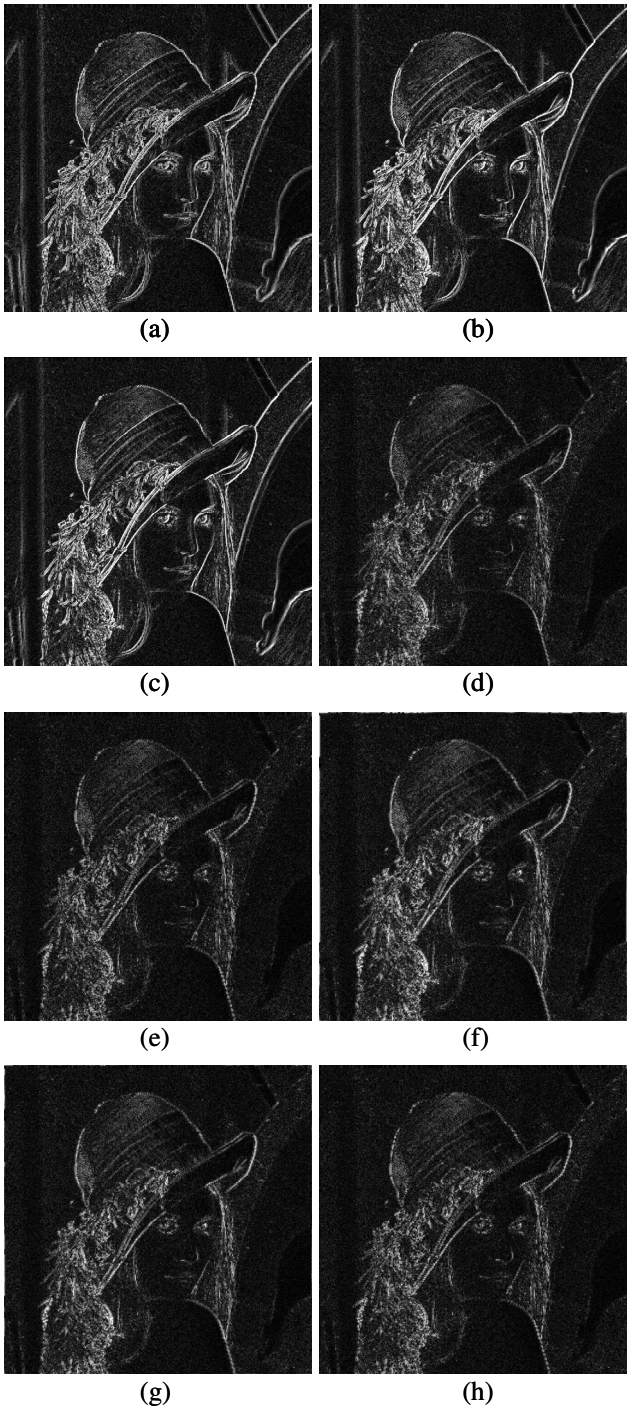

(a) (b) (c) (d) (e) (f) (g) (h)

Figure 4: Difference images magnified by a factor of ten, (a) Nearest neighbourhood, (b) Bilinear, (c) Bicubic, (d) Sinc, (e) Cycle Spinning (CS) [8], (f) Directional Cycle Spinning (DSC) [9], (g) Yinji [4] and (h) the proposed methods.